

# Hydrolysis Precipitation Synthesis of $\text{SnO}_2 \cdot x\text{H}_2\text{O}$ as Electrode Materials for Supercapacitors

Wang Shuyun, Zhao Jiachang, Gao Shuai, Gao Yilong, Liu Xijian, Wu Yuandong, Xu Jingli

Shanghai University of Engineering Science, Shanghai 201620, China

**Abstract:** Electrode materials of  $\text{SnO}_2 \cdot x\text{H}_2\text{O}$  were synthesized by hydrolysis precipitation process. After calcination at various temperatures, the materials were characterized by X-ray diffraction (XRD), transmission electron microscopy (TEM) and thermogravimetric analysis (TGA). XRD patterns confirm that the structure of  $\text{SnO}_2 \cdot x\text{H}_2\text{O}$  is tetragonal (rutile). TEM images reveal the morphology of the  $\text{SnO}_2 \cdot x\text{H}_2\text{O}$ . TGA shows the water content in  $\text{SnO}_2 \cdot x\text{H}_2\text{O}$  decreases as the calcination temperature increases. Electrochemical tests, such as cyclic voltammetry (CV), chronopotentiometry and cycling were also performed to study the supercapacitor behavior of  $\text{SnO}_2 \cdot x\text{H}_2\text{O}$ . CV results indicate that  $\text{SnO}_2 \cdot x\text{H}_2\text{O}$  calcined at 200 °C has a specific capacitance of 36.1 F/g at the scan rate of 5 mV/s in 0.5 mol/L  $\text{H}_2\text{SO}_4$  electrolyte. Cycling test of the same sample also shows excellent long-term cyclic stability, which has lost less than 2% of the total specific capacitance after 2000 cycles. These results indicate that the prepared  $\text{SnO}_2 \cdot x\text{H}_2\text{O}$  materials are excellent candidates as electrode materials for supercapacitors.

**Key words:**  $\text{SnO}_2 \cdot x\text{H}_2\text{O}$ ; hydrolysis precipitation process; supercapacitors; electrochemical performance

Supercapacitors have received great attention in the field of electrochemical energy storage and conversion due to their ability of delivering high levels of electrical power and long cycle life<sup>[1]</sup>. They can be categorized as electric double-layer capacitors (EDLCs) and faradaic pseudo-capacitors. EDLCs use the physical separation of electronic charge in the electrode and ions of the electrolyte adsorbed on the surface of electrode. And an optimal faradaic pseudocapacitors are charged by chemical sorption of a working cation of the electrolyte at a reduced complex at the surface of the electrode<sup>[2]</sup>. Many oxides, such as  $\text{RuO}_2$ <sup>[3]</sup>,  $\text{MnO}_2$ <sup>[4]</sup>,  $\text{NiO}$ <sup>[5]</sup> and  $\text{Co}_3\text{O}_4$ <sup>[6]</sup> have been widely reported in the applications of faradaic pseudo-capacitors due to high specific capacitance.

Tin oxide ( $\text{SnO}_2$ ) is now widely used in catalysis, gas sensors and lithium batteries<sup>[7-9]</sup>. Recent research towards the application of  $\text{SnO}_2$  as supercapacitor materials has also brought much attention to the society. Selvan et al. synthesized  $\text{SnO}_2$  and  $\text{SnO}_2@\text{C}$  by reactions under autogenic pressure at elevated

temperatures, and  $\text{SnO}_2@\text{C}$  has a specific capacitance of 37.8 F/g<sup>[10]</sup>. In the meantime, Wu reported that  $\text{Fe}_3\text{O}_4\text{-SnO}_2$  composites delivered specific capacitance of 33 F/g in  $\text{Na}_2\text{SO}_4$  electrolyte<sup>[11]</sup>. Besides, thin films of  $\text{SnO}_2 \cdot x\text{H}_2\text{O}$  have been synthesized via a simple successive ionic layer adsorption and reaction method, delivering specific capacitance of 25 F/g in  $\text{Na}_2\text{SO}_4$  electrolyte<sup>[12]</sup>. Similarly  $\text{SnO}_2$  thin films were deposited by chemical route, showing specific capacitance of 66 F/g in  $\text{Na}_2\text{SO}_4$  electrolyte<sup>[13]</sup>. While tin oxide thin films were prepared via a spray pyrolysis method, showing specific capacitance of 168 F/g in KOH electrolyte<sup>[14]</sup>. When amorphous tin oxide was potentiodynamically deposited onto stainless steel electrode, a specific capacitance of 285 F/g could be obtained<sup>[15]</sup>. We deduce that  $\text{SnO}_2$  prepared at lower temperature delivers higher specific capacitance. And by comparing other oxides, such as  $\text{RuO}_2$ , the  $\text{SnO}_2$  usually has higher specific capacitance in the form of hydrate.

In the report of Lee et al., strong acid  $\text{H}_2\text{SO}_4$  electrolyte was

Received date: January 21, 2015

Foundation item: Shanghai University of Engineering Science (A-0508-13-01014)

Corresponding author: Zhao Jiachang, Ph. D., Associate Professor, College of Chemistry and Chemical Engineering, Shanghai University of Engineering Science, Shanghai 201620, P. R. China, Tel: 0086-21-67791216, E-mail: zjc@sues.edu.cn

Copyright © 2016, Northwest Institute for Nonferrous Metal Research. Published by Elsevier BV. All rights reserved.

found to be better than mild KCl<sup>[2]</sup>, and SnO<sub>2</sub> was confirmed to be stable in H<sub>2</sub>SO<sub>4</sub> electrolyte<sup>[16]</sup>. In order to improve the electrical conductivity, tin oxide hydrate need to be annealed, but the specific capacitance tends to be low if the temperature is much higher<sup>[17]</sup>. In the present work, SnO<sub>2</sub>·xH<sub>2</sub>O electrode materials have been synthesized by hydrolysis precipitation process and the effect of calcination temperature on the structure and the electrochemical performance of SnO<sub>2</sub>·xH<sub>2</sub>O has been investigated.

## 1 Experiment

SnO<sub>2</sub>·xH<sub>2</sub>O materials were synthesized by adding 144 mL of 2.5 mol/L ammonia solution to 60 mL of 1 mol/L SnCl<sub>4</sub> solution in an ice bath from 0 °C to 4 °C and stirred at around 3000 r/min thoroughly for 4 h. Then the resulting precipitate was collected by centrifugation, and washed several times with ethanol, then dried at 80 °C for 2 h. The precipitate was separated and calcined at 100, 150, 200, 250 and 300 °C for 2 h. The samples obtained were designated as SH-100, SH-150, SH-200, SH-250 and SH-300 accordingly.

XRD analysis was conducted using Deutschland RUKERD2 PHASER X-Ray diffractometer. TEM analysis was carried out with JEOL 2010 microscope. TGA analysis was carried out in N<sub>2</sub> using STAPT-1000 Deutschland LINSEIS thermogravimetric analyzer. The electrode was formed by mixing 75 wt% SnO<sub>2</sub>·xH<sub>2</sub>O, 20 wt% super P, and 5 wt% PTFE as binder. Each of the slurry was then rolled into a thin sheet of titanium mesh. The electrochemical performances of the electrodes were studied in a three-electrode system in 0.5 mol/L H<sub>2</sub>SO<sub>4</sub> electrolyte with CHI660C electrochemical workstation, where the SnO<sub>2</sub>·xH<sub>2</sub>O electrodes, platinum plate and saturated calomel electrode were applied as the working electrode, counter electrode and reference electrode, respectively. The electrochemical performances of SnO<sub>2</sub>·xH<sub>2</sub>O were tested using a CV method, chronopotentiometry and cycling test. The specific capacitance of the electrode can be calculated from the CV curves according to the following equation:

$$C = \frac{Q}{\Delta E \cdot m} \quad (1)$$

where  $C$  (F/g) is the specific capacitance,  $Q$  (C) is the average charge,  $m$  (g) is the mass of the SnO<sub>2</sub>·xH<sub>2</sub>O in the electrode, and  $\Delta E$  (V) represents voltage range.

The capacitance from the constant current charge-discharge curve can be calculated using the following equation:

$$C = \frac{It}{\Delta E \cdot m} \quad (2)$$

where  $I$  (A) represents the total current,  $t$  (s) is the discharge time, the  $\Delta E$  (V) represents potential during constant current discharge.

## 2 Results and Discussion

### 2.1 Structural study, thermal analysis and surface morphology

Fig.1a shows XRD patterns of SnO<sub>2</sub>·xH<sub>2</sub>O at around 26.6°, 33.9°, 51.8°, 64.7°, indexed as (110), (101), (211) and (112) planes, respectively with tetragonal rutile structure SnO<sub>2</sub>, which is corresponding to JCPDS files No.41-1445. It is observed that the peaks are relatively broadened, which further indicates that the materials have low crystallinity. It is noted that the diffraction intensity increases and the full-width at half-maximum (FWHM) of diffraction peaks reduces with the increase of the annealing temperature, revealing the enhancement of the crystallization of the materials.

TGA curves was used to determine the water content of SnO<sub>2</sub>·xH<sub>2</sub>O. It is found in Fig.1b that the SnO<sub>2</sub>·xH<sub>2</sub>O can stabilize to a temperature as high as 500 °C. There are two mass loss steps in the temperature range<sup>[18]</sup>: The first step ends at 175 °C of SH-100, SH-150, SH-200, SH-250 and SH-300 with loss of mass 11%, 10%, 8%, 8%, and 6%, respectively. This effect is reasonably attributed to the absence of physically adsorbed water<sup>[19]</sup>. Then the water content of the SnO<sub>2</sub>·xH<sub>2</sub>O materials is 12wt%, 7wt%, 7wt%, 5wt%, 6wt%, respectively. Theoretical mass loss of SnO<sub>2</sub>·xH<sub>2</sub>O approaches to anhydrous SnO<sub>2</sub>. The above results indicate that percentage content of water in the SnO<sub>2</sub>·xH<sub>2</sub>O decreases as the calcination temperature increases.

The effect of annealing temperature on the morphology of SnO<sub>2</sub>·xH<sub>2</sub>O can be directly observed from the TEM images in Fig.2. SnO<sub>2</sub>·xH<sub>2</sub>O mainly consists of randomly dispersed, spherical particles. The TEM images reveal that the particles are mainly dispersed with submicron size and their outer surfaces are constructed of many small nanoclusters that are rapidly grown from the center of the spheres. The crystallinity of the SnO<sub>2</sub>·xH<sub>2</sub>O also increases with the increase of the temperature.

### 2.2 Electrochemical performance

Fig.3 shows the CV responses of SnO<sub>2</sub>·xH<sub>2</sub>O at the scan rate of 5 mV/s. All curves show rectangular shapes within the measured potential window, indicating a better ideal electrical and good capacitive behavior.

Fig.4 displays cyclic voltammograms of SH-200 in 0.5 mol/L H<sub>2</sub>SO<sub>4</sub> electrolyte at different scan rates. It also can be observed that the response current of the electrode almost reverses instantaneously when the scan direction changes whether from anodic to cathodic scan or from cathodic to

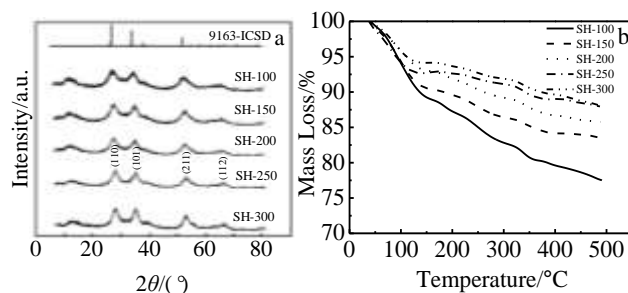


Fig.1 X-ray diffraction patterns (a) and TGA curves (b) of SnO<sub>2</sub>·xH<sub>2</sub>O

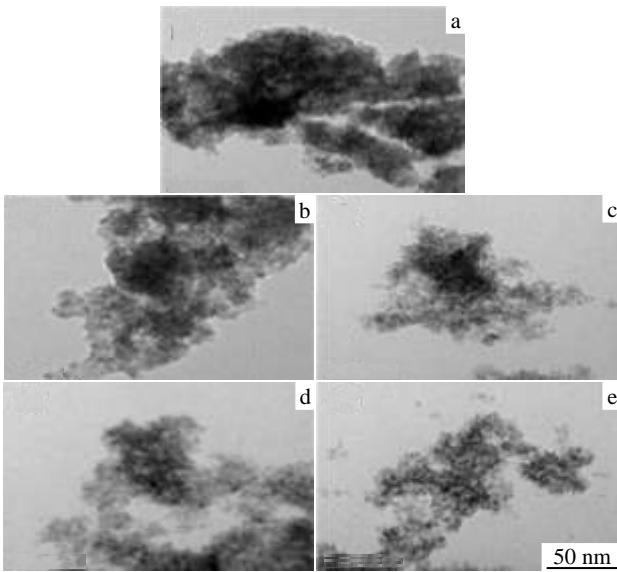


Fig.2 TEM images of SnO<sub>2</sub>·xH<sub>2</sub>O: (a) SH-100, (b) SH-150, (c) SH-200, (d) SH-250, and (e) SH-300

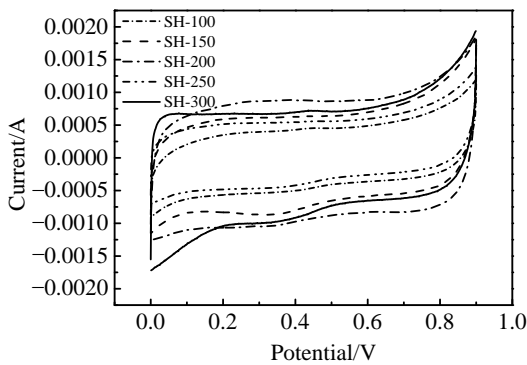


Fig.3 CV curves of SnO<sub>2</sub>·xH<sub>2</sub>O in 0.5 mol/L H<sub>2</sub>SO<sub>4</sub> electrolyte at the scan rate of 5 mV/s

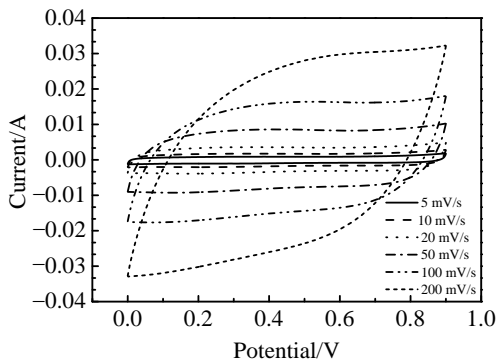


Fig.4 CV curves of SH-200 in 0.5 mol/L H<sub>2</sub>SO<sub>4</sub> electrolyte at different scan rates

anodic scan. And the integral area of CV curves increases with increasing of the scan rate, which indicates that the voltammetric currents are directly proportional to the scan rate<sup>[20]</sup>.

The variation in the specific capacitance calculated from

CV curves of the SnO<sub>2</sub>·xH<sub>2</sub>O as a function of the scan rate is plotted in Fig.5. At the scan rate of 5 mV/s, the specific capacitances of SH-100, SH-150, SH-200, SH-250, and SH-300 reach 18.1, 18.5, 36.1, 26.5 and 23.9 F/g, respectively. The specific capacitance of SH-200 is higher than the reported values of SnO<sub>2</sub> synthesized by wet chemical techniques (5.3 F/g at 25 mV/s in a 0.1 mol/L H<sub>2</sub>SO<sub>4</sub> electrolyte)<sup>[21]</sup>. And the specific capacitance of 19.6 F/g is obtained even at a higher scan rate of 200 mV/s for SH-200, and SH-200 has a higher capacitance value compared with other samples at any scan rate. This comparative decrease in the specific capacitance at higher scan rates is mainly attributed to the increase in ionic resistivity and the ion inaccessibility of the electrode surface at high charging-discharging rates<sup>[22]</sup>. The SH-200 is better because more anhydrous SnO<sub>2</sub> will form when water is irreversibly lost from structure upon annealing in air, resulting in an increase in the metallic conduction paths but a decrease in the volume of protonic transport paths<sup>[23]</sup>.

The charge-discharge behavior of SH-200 was measured by chronopotentiometry from 0 V to 0.9 V at a constant current of 0.005 A and the result is shown in Fig.6a. The specific capacitance of the SnO<sub>2</sub>·xH<sub>2</sub>O derived from the discharge curve is found to be 32.0 F/g at 0.005 A, which is close to the value of 36.1 F/g derived from the cyclic voltammogram at the scan rate of 5 mV/s.

The cycle stability was also investigated over 2000 cycles for SH-200 electrode at a scan rate of 20 mV/s. Fig.6b shows the specific capacitance retention as a function of cycle

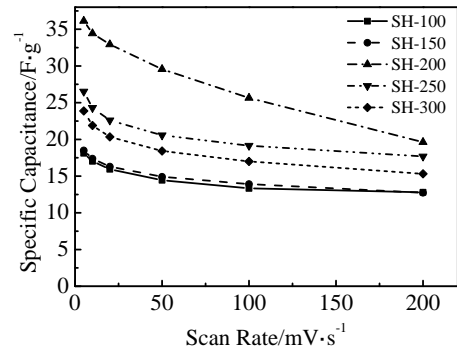


Fig.5 Dependence of specific capacitance of SnO<sub>2</sub>·xH<sub>2</sub>O as a function of scan rates

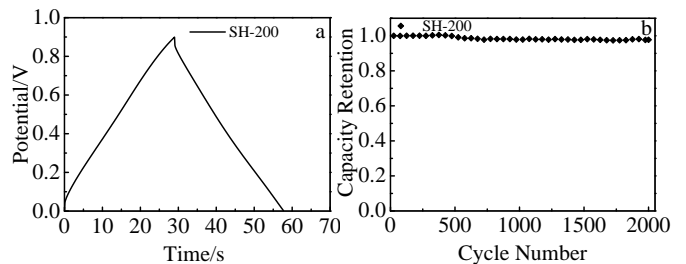


Fig.6 Chronopotentiometry curve of SH-200 at 5 mA in 0.5 mol/L H<sub>2</sub>SO<sub>4</sub> electrolyte (a) and capacity retention of SH-200 in the scan rate of 20 mV/s as a function of cycle number (b)

number. A decrease of 2% of the specific capacitance is observed after 2000 cycles. This long-term electrochemical stability indicates that this kind of material have a long-term electrochemical stability.

### 3 Conclusions

1) Hydrolysis precipitation process is a simple and efficient way to fabricate  $\text{SnO}_2 \cdot x\text{H}_2\text{O}$  electrode materials.

2)  $\text{SnO}_2 \cdot x\text{H}_2\text{O}$  crystallite with a tetragonal rutile structure is formed directly and the crystallinity increases with the increase of temperature. The synthesized materials are determined to be hydrate. The crystallinity and particle size of the  $\text{SnO}_2 \cdot x\text{H}_2\text{O}$  increase with the increase of temperature.

3) The synthesized materials possess typical capacitance behavior within a potential range from 0 to 0.9 V in 0.5 mol/L  $\text{H}_2\text{SO}_4$  electrolyte. The  $\text{SnO}_2 \cdot x\text{H}_2\text{O}$  materials calcined at 200 °C is a suitable candidate for super-capacitors application as it has a specific capacitance of 36.1 F/g. This kind of materials has a long-term electrochemical stability.

### References

- Lang X, Hirata A, Fujita T et al. *Nat Nanotech*[J], 2011, 6: 232
- Lee H Y, Goodenough J B. *J Solid State Chem*[J], 1999, 144: 220
- Conway B E. *J Electrochem Soc*[J], 1991, 138: 1539
- Chen S, Zhu J, Wu X et al. *Acs Nano*[J], 2010, 4: 2822
- Yuan C, Zhang X, Su L et al. *J Mater Chem*[J], 2009, 19: 5772
- Xia X, Tu J, Mai Y et al. *J Mater Chem*[J], 2011, 21: 9319
- Zhang H, Hu C, Chen S et al. *Catal Lett*[J], 2012, 142: 809
- Wang B, Zhu L F, Yang Y H et al. *J Phys Chem C*[J], 2008, 112: 6643
- Ning J, Dai Q, Jiang T et al. *Langmuir*[J], 2008, 25: 1818
- Selvan R K, Perelshtein I, Perkas N et al. *J Phys Chem C*[J], 2008, 112: 1825
- Wu N L. *Mater Chem Phys*[J], 2002, 75: 6
- Pusawale S N, Deshmukh P R, Lokhande C D et al. *Bull Mater Sci*[J], 2011, 34: 1179
- Pusawale S N, Deshmukh P R, Lokhande C D. *Appl Surf Sci*[J], 2011, 257: 9498
- Vijayakumar S, Nagamuthu S, Purushothaman K et al. *Int J Nanoscience*[J], 2011, 10: 1245
- Prasad K R, Miura N. *Electrochem Commun*[J], 2004, 6: 849
- Wang W, Hao Q, Lei W et al. *RSC Adv*[J], 2012, 2: 10 268
- Long W J, Swider K E, Merzbacher C I et al. *Langmuir*[J], 1999, 15: 780
- Khalaf H A, El-Madani E A, Mansour S E et al. *Global J Inorg Chem*[J], 2011, 2: 102
- Magnacca G, Cerrato G, Morterra C et al. *Chem Mater*[J], 2003, 15: 675
- Gujar T, Shinde V, Lokhande C et al. *J Power Sources*[J], 2006, 161: 1479
- Hu C C, Wang C C, Chang K H. *Electrochim Acta*[J], 2007, 52 : 2691
- Rudge A, Davey J, Raistrick I et al. *J Power Sources*[J], 1994, 47: 89
- Chang K H, Hu C C, Chou C Y. *Electrochim Acta*[J], 2009, 54: 978

## 水解沉淀法制备超级电容器 $\text{SnO}_2 \cdot x\text{H}_2\text{O}$ 电极材料

王淑云, 赵家昌, 高 帅, 高艺茏, 刘锡建, 吴远东, 徐菁利  
(上海工程技术大学, 上海 201620)

**摘 要:** 采用水解沉淀法制备  $\text{SnO}_2 \cdot x\text{H}_2\text{O}$  电极材料。经过不同温度的焙烧, 将得到的  $\text{SnO}_2 \cdot x\text{H}_2\text{O}$  电极材料用 X 射线粉末衍射 (XRD), 透射电子显微镜 (TEM) 和热失重测试 (TGA) 进行分析。XRD 测试表明,  $\text{SnO}_2 \cdot x\text{H}_2\text{O}$  电极材料为金红石结构。TEM 证实了  $\text{SnO}_2 \cdot x\text{H}_2\text{O}$  的形貌。TGA 表明, 随着焙烧温度的升高,  $\text{SnO}_2 \cdot x\text{H}_2\text{O}$  含水量降低。通过循环伏安法, 恒流充放电和循环寿命研究了  $\text{SnO}_2 \cdot x\text{H}_2\text{O}$  的电化学行为。CV 测试表明, 在 200 °C 下焙烧的  $\text{SnO}_2 \cdot x\text{H}_2\text{O}$  电极材料在 5 mV/s, 0.5 mol/L  $\text{H}_2\text{SO}_4$  中的比电容为 36.1 F/g。经过 2000 次循环后, 比电容与首次循环的比电容相比减少了 2%。这些结果表明用化学沉淀法制备的  $\text{SnO}_2 \cdot x\text{H}_2\text{O}$  是超级电容器良好的候选材料。

**关键词:**  $\text{SnO}_2 \cdot x\text{H}_2\text{O}$ ; 水解沉淀法; 超级电容器; 电化学性能

作者简介: 王淑云, 女, 1988 年生, 硕士生, 上海工程技术大学化学化工学院, 上海 201620, 电话: 021-67791216, E-mail: wangshuyun306@126.com.cn